J Supercond Nov Magn (2016) 29:803–808
DOI 10.1007/s10948-015-3355-4

ORIGINAL PAPER

Enhanced Microwave Absorbing Properties of La^{3+} Substituting Barium Hexaferrite

Yankui Cheng[1] · **Xiaohu Ren**[2]

Received: 6 October 2015 / Accepted: 17 December 2015 / Published online: 4 January 2016

Abstract Barium hexagonal ferrites doped with La^{3+}, $Ba_{1-x}La_xCoTiFe_{10}O_{19}$ ($x = 0.10, 0.15, 0.20$), were prepared by sol-gel combustion method. The structure, magnetic properties, and microwave absorption of the samples were investigated. The X-ray diffraction patterns of the doped ferrites confirmed the formation of the M-type barium ferrite, and no other impurities could be found. The electromagnetic parameter spectra showed that The La^{3+} ions doped in the ferrite improved complex permittivity and permeability so that microwave absorption was enhanced. The minimum reflection loss of −39.15 dB was obtained for sample $x = 0.20$ with thickness of 2.4 mm, and the maximum bandwidth of RL< −10 dB can reach to 11.5 GHz when the thickness is 2.0 mm.

Keywords Barium ferrite · Microwave absorption · Wideband · Reflection loss

1 Introduction

The rapid developments of electrical and electronic devices cause a growing request in microwave absorbing materials, which could be used extensively in commerce, industry, and defense applications [1–6]. Due to their strong absorption of electromagnetic (EM) wave, the microwave absorbers can minimize various EM radiations and interferences. In this way, an appropriate microwave absorber can eliminate the excessive electromagnetic waves to ensure the people's health and the undisturbed functioning of equipment. Moreover, the appropriate absorbers can help military aircrafts and vehicles to avoid detection by the radar in defense and aerospace industries, as the application of microwave absorbing coating on the exterior surfaces of military equipments. However, owing to the advancing technology, the EM wave absorbing materials are expected to have broad bandwidth, minimum reflection loss (RL), and light weight (or small thickness) in recent years [7]. Therefore, broadening bandwidth and minimizing reflection loss have been the vital problem for microwave absorbers.

Among the microwave absorbing materials, M-type barium hexagonal ferrite ($BaFe_{12}O_{19}$, BaM) has generated considerable recent research interests because of its low cost, good stability, large magnetocrystalline anisotropy, high natural resonance frequency (about 47.6 GHz), and excellent magnetic loss [7–10]. At the microwave band, the microwave attenuation properties of BaM are closely related to the magnetic losses which result mainly from the resonance absorption of moving magnetic domains in lower frequency and the spin relaxation of magnetization in higher frequency. It has been known that the microwave absorption performance can be improved by choosing suitable cations to substitute the Fe^{3+} in BaM. M. K. Tehrani et al. [11] have confirmed that the bandwidth of EM wave absorption for BaM can be broadened when the Fe^{3+} was partially replaced by metal cations (Mg^{2+}, Mn^{2+}, Co^{2+}) and Ti^{4+}. C. S. Dong et al. [12] have demonstrated that the minimum reflection loss of $BaCo_{0.3}Ti_{0.3}$ $Fe_{11.4}O_{19}$ can reach −47 dB at the thickness of 0.8 mm. X. Tang and his co-workers [13] have reported that the non-stoichiometric Ni^{2+}-Ti^{4+}

✉ Xiaohu Ren
kk123oo@126.com

[1] Department of Modern Manufacturing, Yibin Vocational and Technical College, Yibin 644003, China

[2] State Key Laboratory of Solidification Processing, School of Materials Science and Engineering, Northwestern Polytechnical University, Xi'an 710072, China

can improve the absorption performance of BaM and the natural resonance frequency of the doped ferrite shift to X-band (8–12 GHz). Thus, using the right cations to substitute BaM is significant for the excellent microwave absorption properties of the absorbing materials. However, influence of substituting Ba^{2+} on properties of barium hexaferrite has been rarely reported.

In the current work, the La^{3+}-doped ferrites $Ba_{1-x}La_xCoTiFe_{10}O_{19}$ were synthesized and the phase composition was confirmed. Moreover, the magnetic and microwave absorption properties were investigated in the frequency range of 2–18 GHz.

2 Experimental

The powders of $Ba_{1-x}La_xCoTiFe_{10}O_{19}$ (x=0.10, 0.15, 0.20) were synthesized via the sol-gel combustion method. As starting materials, stoichiometric amount of $Fe(NO_3)_3{\cdot}9H_2O$, $Ba(NO_3)_2$, $Co(NO_3)_2{\cdot}6H_2O$, $Ti(OC_4H_9)_4$, and $La(NO_3)_3{\cdot}6H_2O$ were dissolved in deionized water by stirring it constantly using a magnetic stirrer. After dissolved completely, appropriate citric acid solution was added into the solution, and then ammonia solution was added dropwise with vigorous stirring to maintain the pH value of the solution at 7. Subsequently, the neutralized solution was heated at 100°C with continuous magnetic stirring to obtain the dried gel. With further heating, the dried gel would burn up in a self-propagating combustion manner, and some brown precursors could be obtained. Finally, the precursors were pre-heated at 450 °C for 2 h and then calcined at 1100 °C for 4 h to obtain the ferrite powders.

The phase composition of ferrites was identified by the X-ray diffractometer (XRD; PANalytical X'Pert PRO), with Cu Kα radiation ($\lambda = 1.540598$ Å) in the range of 20°–75°. The morphology was observed by using the field emission scanning electron microscopy (FE-SEM; Zeiss Ultra 55). The vibrating sample magnetometer (VSM) was used to measure magnetic properties of the ferrites at room temperature. The resulting ferrite powders were mixed with paraffin wax at ratio of 6:1 and then compacted into a circular cylinder with the inner diameter of 3.04 mm, the outer diameter of 7.0 mm. The electromagnetic parameters of composite samples in the frequency range of 1–18 GHz were measured by network analyzer (Agilent Technologies, E8363A) using a coaxial method.

3 Results and Discussion

The X-ray diffraction patterns of $Ba_{1-x}La_xCoTiFe_{10}O_{19}$ (x=0.10, 0.15, 0.20) are presented in Fig. 1. The results show that all the samples have similar diffraction patterns

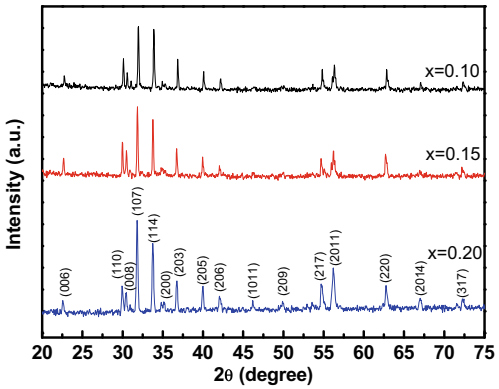

Fig. 1 The X-ray patterns for $Ba_{1-x}La_xCoTiFe_{10}O_{19}$ with $x = 0.10$, 0.15, and 0.20

representing a single phase with hexagonal crystal structure and no second phase can be found, indicating that the La^{3+} can enter the lattice and do not affect the crystal structure of hexagonal barium ferrite. However, the substitution of Ba^{2+} with La^{3+} results in a slight change of diffraction peak position due to the slight change in lattice parameters of the respective compounds. The lattice parameters (a and c) are tabulated in Table 1 and which were calculated by the following formula:

$$d = \frac{1}{\sqrt{4(h^2 + hk + k^2)/3a^2 + l^2/c^2}} \quad (1)$$

where (hkl) is the Miller indices, and d is the crystal face distance. It can be seen that the value of a decreases little, the value of c decreases from 23.423 to 23.136 Å and the ratio of c/a decreases from 3.954 to 3.913 with increasing x. The variations of lattice parameters can be attributed to partial replacement of Ba^{2+} (ionic radius 149 pm) with the smaller La^{3+} (ionic radius 117 pm) ions.

A representative scanning electron micrograph (SEM) for $Ba_{0.8}La_{0.2}CoTiFe_{10}O_{19}$ is shown in Fig. 2. The micrograph clearly illustrates hexagonal structure. From the image, it can be seen that the particles appear fine grain growth with the grains size varying from 100 to 300 nm. The micrographs of other samples also show similar features and no obvious microstructure change is seen with La^{3+} substitution.

The magnetic hysteresis loops for $Ba_{1-x}La_xCoTiFe_{10}O_{19}$ with different values of x are shown in Fig. 3. The saturation magnetization $M_s$and coercivity H_c are

Table 1 Lattice parameters for all compositions

Sample	Chemical formula	a (Å)	c (Å)	c/a
x= 0.10	$Ba_{0.8}La_{0.2}CoTiFe_{10}O_{19}$	5.923	23.423	3.954
x= 0.15	$Ba_{0.85}La_{0.15}CoTiFe_{10}O_{19}$	5.917	23.291	3.936
x= 0.20	$Ba_{0.9}La_{0.1}CoTiFe_{10}O_{19}$	5.912	23.136	3.913

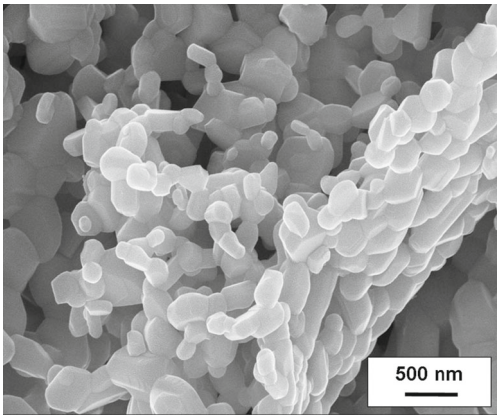

Fig. 2 Scanning electron micrograph (SEM) for sample with x= 0.20

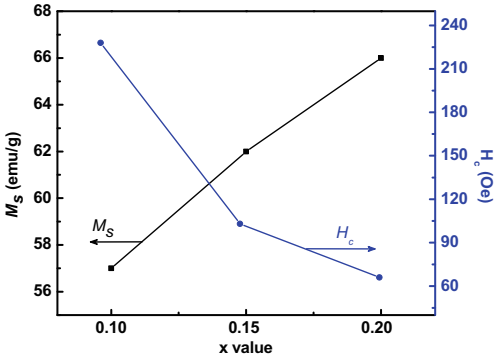

Fig. 4 Saturation magnetization M_s and coercivity H_c of $Ba_{1-x}La_xCoTiFe_{10}O_{19}$

plotted in Fig. 4 as a function of La^{3+} substitution. The hysteresis loops show that all the samples exhibit typical characteristics of soft magnetic materials. The value of M_s increases from 57 to 66 emu/g with increasing La^{3+} amount as revealed in Fig. 4. On the contrary, the value of $H_c$decreases with increasing x. These can be explained by the ferromagnetic theory of ferrite. The increase of M_s is ascribed to the occupation of La^{3+} in the lattice site of Ba^{2+} enhancing molecular magnetic moment, and the decease of H_c is due to the weakened uniaxial magnetocrystalline anisotropy of the barium ferrite for La^{3+} substitution being consistent with variation of lattice parameter c/a.

In order to understand the possible microwave absorption mechanism, the complex permittivity ($\varepsilon_r = \varepsilon' - j\varepsilon''$) and complex permeability ($\mu_r = \mu' - j\mu''$) were investigated. The complex permittivity and complex permeability can be used to represent the dielectric and dynamic magnetic properties of materials. For microwave absorber, the real part of complex permittivity and permeability is proportional to storage capability of electric and magnetic energy when the material is under an applied electric or magnetic field. The

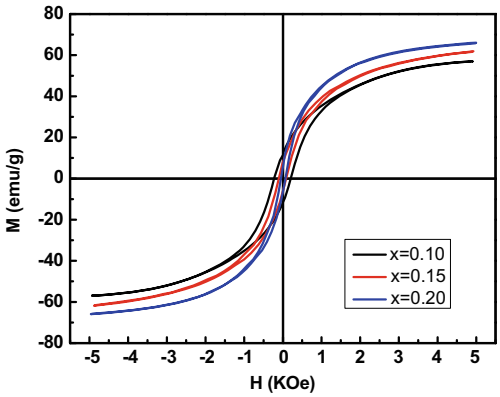

Fig. 3 Magnetic hysteresis loops for the $Ba_{1-x}La_xCoTiFe_{10}O_{19}$ with x= 0.10, 0.15, and 0.20

imaginary part represents the loss of electric and magnetic energy.

Figure 5 shows the frequency dependence of the real and imaginary parts of the permittivity for $Ba_{1-x}La_xCoTiFe_{10}O_{19}$ samples over the frequency range 1–18 GHz. From Fig. 5a, we can see that the real part (ε') of complex permittivity exhibits indistinctive variation with frequency for all compositions; this is a normal dielectric behavior of ferrites, which was consistent with reported before [14]. However, the value of ε'' shows strong frequency dispersion, which can be attributed to intrinsic electric dipole polarization and interfacial polarization. Furthermore, with the amount of doped La^{3+} increasing, the average value of ε' and ε'' rises continuously. In barium hexaferrites, Ba^{2+} are partially replaced when La^{3+} enter into the lattice, resulting in partial conversion of Fe^{3+} into Fe^{2+} in order to keeping charge equilibrium [15]. Since dielectric polarization mechanism is closely associated with electron hopping mechanism in ferrites, the greater electron hopping chance between Fe^{3+} and Fe^{2+} is the higher the permittivity would be [16]. As a result, the real part of complex permittivity and imaginary part increase with more addition of La^{3+} amount.

Figure 6 shows the frequency dependence of the real (μ') and imaginary (μ'') parts of the permeability for $Ba_{1-x}La_xCoTiFe_{10}O_{19}$. All curves of μ'' vs. frequency had a broad peak corresponding to natural ferromagnetic resonance (f_r), and the peak shift to lower frequency with increasing amount of doped La^{3+}. This can be ascribed to weakening uniaxial magnetocrystalline anisotropy. Above f_r, the real parts of permeability falls sharply to unity. As we mentioned above, the partial Fe^{3+} ions convert to Fe^{2+} ions with increase in La^{3+} content. It is well known that the static magnetic moment of Fe^{2+} (4 μ_B) is lower than that of Fe^{3+} (5 μ_B), resulting in overall magnetic interaction weakening in ferrites, thereby decreasing the values of μ' and μ'' with increasing La^{3+} content. However, as shown in permeability spectra, the values of μ' and μ'' increase slightly

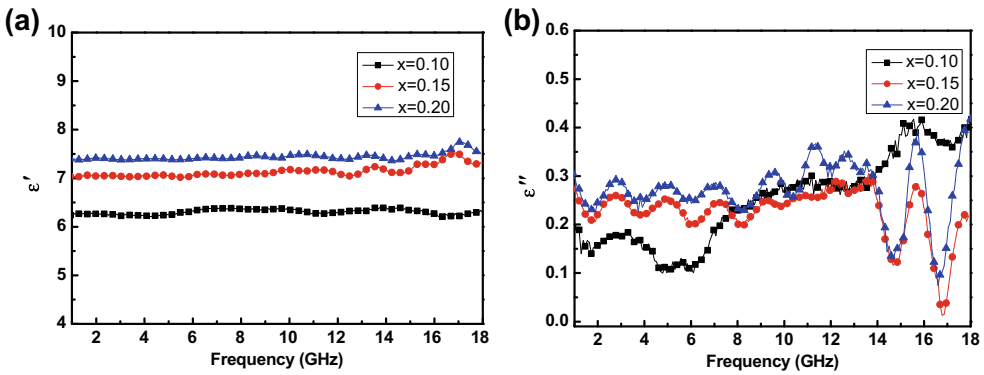

Fig. 5 Frequency dependence of the real (**a**) and imaginary part (**b**) of the complex permittivity for $Ba_{1-x}La_xCoTiFe_{10}O_{19}$(x= 0.10, 0.15, 0.20)

with increasing La^{3+} content instead of decreasing. According to Snoek's law [17], a change in .μ due to variations in material structure is followed by an opposite change in resonance frequency (f_r), i.e., $(\mu_s - 1)f_r = (2/3)(\gamma 4\pi M_s)$, where $4\pi M_s$ is the saturation magnetization, γ is gyromagnetic ratio. As shown in hysteresis loops above,M_s is enhanced with increasing La^{3+} content. Therefore, the value of μ' increases with more addition of La^{3+} amount below f_r.

From the complex relative permittivity and the complex relative permeability, the microwave absorption performance of $Ba_{1-x}La_xCoTiFe_{10}O_{19}$ composites with paraffin wax was investigated. The reflection loss (RL) can be calculated from the relative complex permeability and permittivity with a given frequency range and a given absorber thickness (d) by the following equation [18]:

$$RL = 20\log|(Z_{in} - 1)/(Z_{in} + 1)| \quad (2)$$

Z_{in} is determined as

$$Z_{in} = (\mu_r/\varepsilon_r)^{1/2}\tanh[j(2\pi fd/c)(\mu_r\varepsilon_r)^{1/2}] \quad (3)$$

where Z_{in} is the input impedance of absorber, $\varepsilon_r$and μ_r are complex permittivity and permeability of the composite, respectively, f is the microwave frequency, and c is the velocity of light in free space.

The frequency dependences of RL for all composition with different thicknesses are exhibited in Fig. 7. It is clear that the matching frequency decreases with increase in value of x. As shown in reflectivity curves, two absorption peaks with significantly different values and positions appear for samples with x= 0.15 and x=0.20 at all different thickness. This dispersion can be attributed to domain wall motion at the lower frequency and spin resonance at the higher frequency. However, there is only one absorption peak for composition $x = 0.10$ due to its peak from spin resonance beyond measuring frequency. For the sample $x = 0.10$, the matching frequencies are equal to 14.7 GHz with a minimum RL of −28.36 dB, and the corresponding matching thickness is 2.0 mm. For the sample $x = 0.15$, the RL values of −29.84 and −21.85 dB were achieved in the matching frequencies of 9.16 and 15.6 GHz, respectively. The corresponding value of matching thickness is 2.0 mm. Sample x=0.20 with matching thickness of 2.4 mm exhibits a minimum RL of −39.15 dB at 7.41 GHz. It is notable that the bandwidth of RL¡−10 dB covers entirely X-band (8˜12 GHz) and Ku-band (12˜18 GHz) for sample $x = 0.20$ when matching thickness is 2.0 mm. The obtained results indicate that La^{3+} substituting not only enhance microwave attenuation of barium hexaferrites but also broaden its bandwidth.

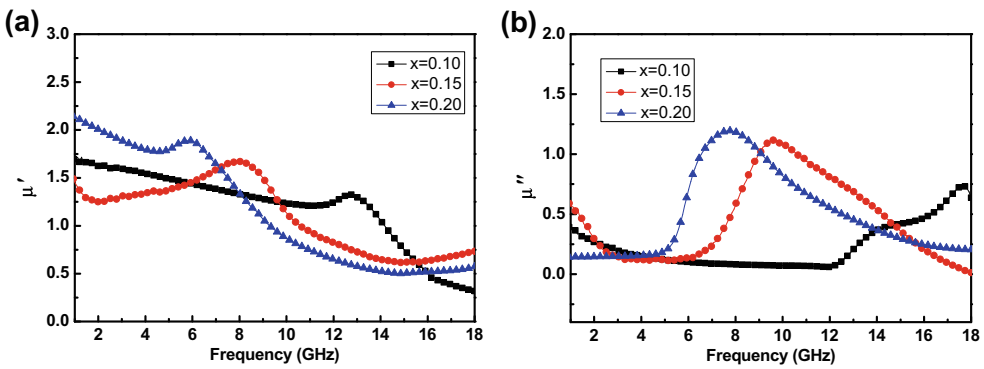

Fig. 6 Frequency dependence of the real (**a**) and imaginary part (**b**) of the complex permeability for $Ba_{1-x}La_xCoTiFe_{10}O_{19}$(x= 0.10, 0.15, 0.20)

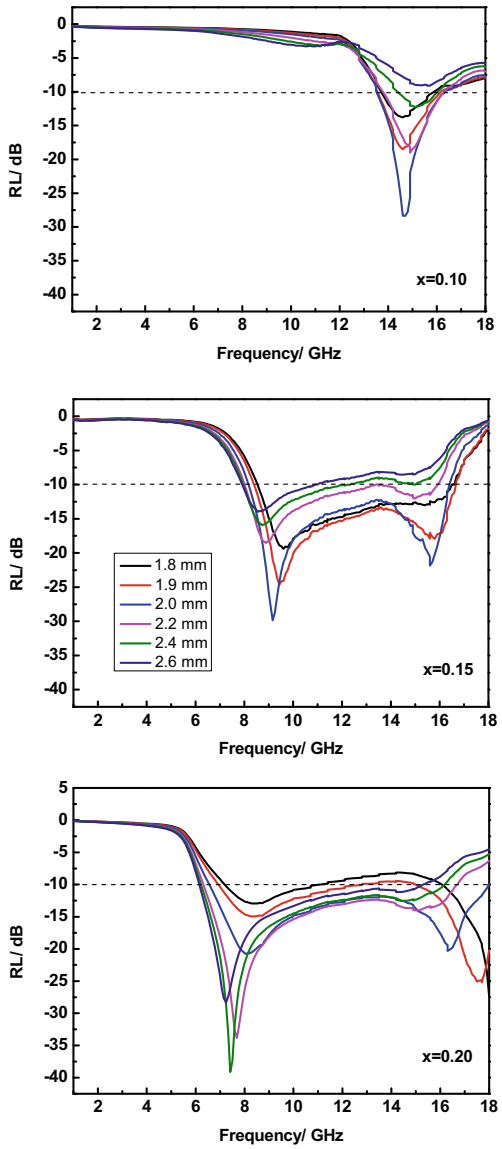

Fig. 7 Frequency dependence of RL for $Ba_{1-x}La_xCoTiFe_{10}O_{19}$ (x=0.10, 0.15, 0.20) at different thicknes

4 Conclusions

In conclusion, Lanthanum ion-doped barium hexaferrites $Ba_{1-x}La_xCoTiFe_{10}O_{19}$ ($x = 0.10, 0.15, 0.20$) have been fabricated successfully by the sol-gel combustion method. The high-frequency magnetic and dielectric properties can be enhanced as addition of La^{3+}. Increasing of La^{3+} content leads to a significant increase in complex permittivity and permeability, while the resonance frequency is shifted to low frequency. Thus, with the incorporation of La^{3+} the absorbing peak moved to the lower frequency and the microwave absorption performance is significantly improved. The sample $Ba_{0.8}La_{0.2}CoTiFe_{10}O_{19}$ has the best microwave absorption performance. The maximum RL of −39.15 dB can be achieved at 7.41 GHz when the matching thickness is 2.4 mm. Furthermore, the maximum bandwidth of RL¡−10 dB can reach to 11.5 GHz (6.5˜18 GHz) when the matching thickness is 2.0 mm.

References

1. Yang, H., Cao, M.S., Y. L, Shi, H.L., Hou, Z.L., Fang, X.Y., Jin, H.B., Wan, W.Z., Yuan, J.: Enhanced dielectric properties and excellent microwave absorption of SiC powders driven with NiO nanorings. Advance Optical Materials **2**, 214–219 (2014)
2. Wang, Y., Huang, Y., Ding, J.: Synthesis and enhanced electromagnetic absorption properties of polypyrrole–$BaFe_{12}O_{19}$/$Ni_{0.8}Zn_{0.2}Fe_2O_4$ on graphene nanosheet. Synth. Met. **196**, 125–130 (2014)
3. Singh, A.P., Mishra, M., Sambyal, P., Gupta, B.K., Singh, B.P., Chandrad, A., Dhawan, S.K.: Encapsulation of γ-Fe_2O_3 decorated reduced graphene oxide in polyaniline core–shell tubes as an exceptional tracker for electromagnetic environmental pollution. J. Mater. Chem. A **2**, 3581–3593 (2014)
4. Baniasadi, A., Ghasemi, A., Nemati, A., Ghadikolaei, M.A., Paimozd, E.: Effect of Ti–Zn substitution on structural, magnetic and microwave absorption characteristics of strontium hexaferrite. J. Alloys Compd. **583**, 325–328 (2014)
5. Wang, Y.M., Wang, L.D., Wu, H.J.: Enhanced microwave absorption properties of α-Fe_2O_3-filled ordered mesoporous carbon nanorods. Materials **6**, 1520–1529 (2013)
6. Liu, P.B., Huang, Y., Wang, L., Zhang, W.: Preparation and excellent microwave absorption property of three component nanocomposites: polyaniline-reduced grapheme oxide-Co_3O_4 nanoparticles. Synth. Met. **177**, 89–93 (2013)
7. Kong, L.B., Li, Z.W., Liu, L., Huang, R., Abshinova, M., Yang, Z.H., Tang, C.B., Tang, P.K., Deng, C.R., Matitsine, S.: Recent progress in some composite materials and structures for specific electromagnetic applications. Int. Mater. Rev. **58**, 203–259 (2013)
8. Li, L.C., Chen, K.Y., Liu, H., Tong, G.X., Qian, H.S., Hao, B.: Attractive microwave-absorbing properties of M-$BaFe_{12}O_{19}$ ferrite. J. Alloys Compd. **557**, 11–17 (2013)
9. Zhang, W.J., Bai, Y., Han, X., Wang, L., Lu, X.F., Qiao, L.J.: Magnetic properties of Co-Ti substituted barium hexaferrite. J. Alloys Compd. **546**, 234–238 (2013)
10. Xu, F.F., Ma, L., Gan, M.Y., Tang, J.H., Li, Z.T., Zheng, J.Y., Zhang, J., Xie, S., Yin, H., Shen, X.Y., Hu, J.L., Zhang, F.: Preparation and characterization of chiral polyaniline/barium hexaferrite composite with enhanced microwave absorbing properties. J. Alloys Compd. **593**, 24–29 (2014)
11. Tehrani, M.K., Ghasemi, A., Moradi, M., Alam, R.S.: Wideband electromagnetic wave absorber using doped barium hexaferrite in Ku-band. J. Alloys Compd. **509**, 8398–8400 (2011)
12. Dong, C.S., Wang, X., Zhou, P.H., Liu, T., Xie, J.L., Deng, L.J.: Microwave magnetic and absorption properties of M-type ferrite $BaCo_xTi_xFe_{12-2x}O_{19}$ in the Ka band. J. Alloys Compd. **354**, 340–344 (2014)
13. Tang, X., Yang, Y.G., Hu, K.: Structure and electromagnetic behavior of $BaFe_{12-2x}(Ni_{0.8}Ti_{0.7})xO_{19-0.8x}$ in the 2–12 GHz frequency range. J. Alloys Compd. **477**, 488–492 (2009)
14. Meng, P.Y., Xiong, K., Wang, L., Li, S.N., Cheng, Y.K., Xu, G.L.: Tunable complex permeability and enhanced microwave absorption properties of $BaNi_xCo_{1-x}TiFe_{10}O_{19}$. J. Alloys Compd. **628**, 75–80 (2015)
15. Meena, R.S., Bhattachrya, S., Chatterjee, R.: Complex permittivity, permeability and wide band microwave absorbing property of

La3+ substituted U-type hexaferrite. J. Magn. Magn. Mater. **322**, 1923–1928 (2010)
16. Xu, J.J., Yang, C.M., Zou, H.F., Song, Y.H., Gao, G.M., An, B.C., Gan, S.C.: Electromagnetic and microwave absorbing properties of Co_2Z-type hexaferrites doped with La3+. J. Magn. Magn. Mater. **321**, 3231–3235 (2009)
17. Lagarkov, A.N., Rozanov, K.N.: High-frequency behavior of magnetic composites. J. Magn. Magn. Mater. **321**, 2082–2092 (2009)
18. Ren, X., Xu, G.: Electromagnetic and microwave absorbing properties of NiCoZn-ferrites doped with La^{3+}. J. Magn. Magn. Mater. **354**, 44–48 (2014)